Energy and Spectrum Efficient Blind Equalization with Unknown Constellation for Air-to-Ground Multipath UAV Communications

Mingqian Liu, *Member, IEEE,* Nan Qu, Bodong Shang, Yunfei Chen, *Senior Member, IEEE,* and Fengkui Gong, *Member, IEEE*

***Abstract*—In unmanned aerial vehicle (UAV) communications, frequency-selective fading can severely deteriorate the quality of transmitted signal by generating undesired and disordered constellation diagrams due to scatters in the air-to-ground (ATG) mutipath channels. In this paper, we propose a low-overhead blind equalization method to combat frequency-selective fading in air-ground multipath UAV channels. Specifically, a pre-equalization method is proposed based on a constant modulus algorithm to restore the contour of the constellation diagram. Moreover, the similarity measure function and the difference measure function are derived using template matching to identify the constellation of M-ary quadrature amplitude modulation. Furthermore, we propose a weighted constant cross algorithm (WXA) to reduce the residual mean square error and construct a cross-shaped modulus value, by utilizing the statistical information of the identified normalized standard constellation diagrams and the equalizer output decision symbols' weighting value. The proposed method requires less information and no training sequences and pilots, therefore, if achieves energy and spectrum efficient ATG multipath UAV communications. Simulation results show that the proposed WXA algorithm can reduce the residual mean square error convergence value between -22dB and -25dB, making it very useful for the equalization of the frequency-selective fading channel in typical UAV communication scenarios.**

***Index Terms*—Blind equalization, constellation identification, green communications, multiple quadrature amplitude modulation, unmanned aerial vehicle**

I. Introduction

In wireless communications, unmanned aerial vehicles (UAV) have attracted significant attention in recent years, it can be applied to many fields, such as relaying, surveillance, and remote sensing, etc. [1]-[2]. The transmitted signal in UAV communication has a high probability of experiencing the multipath frequency-selective fading originated from the obstacles in air-to-ground (ATG) channels, such as buildings and trees. This frequency-selectivity can severely deteriorate the quality of the transmitted signal by generating undesired constellation diagrams, especially if the transmission is of large bandwidth. To improve the spectrum efficient, quadrature amplitude modulation (QAM) is offer used to modulate the signal's amplitude and phase [3]. QAM serves as one of the critical technologies in the fifth-generation (5G) and beyond 5G communication systems. However, when the energy is fixed, QAM leads to a smaller distance between constellation points on the normalized constellation diagram, and thus the processing complexity at receivers increases [4]. As a bandwidth saving method, blind equalization can effectively compensate for the distortion induced by the signal in frequency-selective fading channels. Nevertheless, there are still some problems in the blind equalization algorithm, such as slow convergence, sensitivity to channel parameters, etc. Choosing different parameters for the blind equalization algorithm of different M-ary quadrature amplitude modulation (MQAM) modulation types can effectively improve the equalization performance [5].

The constellation identification of QAM over frequency-selective fading channels is essential in signal processing [6]. For the QAM constellation identification, [7] employed high-order cumulants and signal cyclostationarity to identify 4/16/64QAM. Reference [8] adopted the Wigner-Ville distribution (WVD) time-frequency to transform the incoming signal, calculate the signal's Renyi entropy, and then leverage the Dempster-Shafer theory to identify the QAM. Reference [9] proposed a high-order cumulant-based modulation method to determine the digital modulation type of 16/64QAM. In [10], authors introduced a QAM signal constellation identification method based on subtractive clustering. Reference [11] utilized the constellation diagram to identify the QAM. However, most of these works assumed the white Gaussian noise. In addition, most of they are only applicable to square or cross-shaped constellation for QAM. The MIL-STD-188-110C circular constellations identification and the QAM to circular isomorphic (QCI) constellations identification have not been studied.

On the other hand, following the "Sato algorithm" proposed, blind equalization has been the focus of many researchers. It can be mainly divided into three categories. The first category uses high-order statistics features, but these algorithms have

This work was supported by the National Natural Science Foundation of China under Grant 62071364, in part by the Aeronautical Science Foundation of China under Grant 2020Z073081001, in part by the Fundamental Research Funds for the Central Universities under Grant JB210104, and in part by the 111 Project under Grant B08038. This paper will be presented in part at the 2021 17th International Wireless Communications and Mobile Computing Conference (IWCMC 2021). *(Corresponding author: Nan Qu.)*

M. Liu, N. Qu and F. Gong are with the State Key Laboratory of Integrated Service Networks, Xidian University, Shaanxi, Xi'an 710071, China (e-mail: mqliu@mail.xidian.edu.cn; nqu@stu.xidian.edu.cn; fkgong@xidian.edu.cn).

B. Shang is with the Bradley Department of Electrical and Computer Engineering, Virginia Tech, Blacksburg, VA 24060, USA (e-mail: bdshang@vt.edu).

Y. Chen is with the School of Engineering, University of Warwick, Coventry, West Midlands United Kingdom of Great Britain and Northern Ireland CV4 7AL (e-mail: yunfei.chen@warwick.ac.uk).

high computational complexity and are not widely used in practice. The second category uses neural networks, which arises in recent years, and the research is still in the initial stage. The third category uses the Bussgang blind equalization algorithms, where many scholars have been proposed various improved algorithms based on the constant modulus algorithm (CMA). Regarding the blind equalization of square QAM, [12] introduced a minimum fourth-order moment (LMF) algorithm to the equalizer's tap coefficient iterative formula and obtained a desirable equalization performance based on the CMA. Also, [13] introduced an efficient soft-decision algorithm (SDDA) and improved the Newton method for blind equalization of 4QAM. In [14], authors studied the space-time blind equalization (BE) of high-throughput QAM signals in MIMO systems and overcame the local convergence problem by multi-stage processing. Reference [15] proposed a double-blind equalization technique based on rectangular quadrature amplitude modulation (RQAM), namely a rectangular contour algorithm and an improved rectangular contour algorithm. Specifically, the dispersion of the rectangular zero-error contour constants was minimized, and the multi-level processing method was used to overcome the local convergence problem. Also, [16] introduced a robust learning machine framework for single hidden layer feed-forward neural networks (SLFNs). Combined with theoretical discussion, it proposed a single implicit neural network (SLFNs) suitable for blind equalization applications. For the blind equalization of the cross-type constellation diagram, S. Abrar et al. proposed the generalized cross contour algorithm (GCRCA) to improve the generalized square contour algorithm (GSCA). The new cost function includes the modulus and phase information of the equalizer output and can also perform moderate carrier phase recovery [17]. Shafayat Abrar et al. proposed a constant cross algorithm (CXA) and sliced constant cross algorithm (SCXA) and used residual inter-symbol interference and excess mean square error (EMSE) to measure the pros and cons of the algorithm [18]. SCXA and CXA algorithms were superior to the CMA. LIU et al. [19] proposed the improved CXA algorithm on the CXA. The stop-and-go technique was introduced in the weight update to ensure convergence, and the constellation matched error (CME) function was added to the cost function. The modified but improved CXA was proposed to speed up the convergence. These works have provided useful insights on MQAM blind equalization designs, but most of them focus on a specific shape constellation. Moreover, they assume a known modulation method and a type of constellation.

Motivates these observations, this paper proposes a novel energy and spectrum efficient blind equalization algorithm for MQAM with the unknown constellation. The main contributions of this paper are summarized as follows:

- We introduce the concept of pre-equalization to restore the outline of the constellation. The similarity measure function and the difference measure function are established to identify the constellation diagrams of 16/32/64QAM different shapes using the template matching.
- We propose a weighted constant cross algorithm (WXA), which leverages the statistical information of the received signal constellation points and the equalizer output decision symbol weight when constructing the cross-shaped modulus value. This reduces the residual mean square error. Moreover, different parameters are matched for the identified normalized standard constellation diagrams.
- The proposed method requires only a small amount of information without training sequences and pilots, therefore achieving energy and spectrum efficient air-ground multipath UAV communications.

The rest of this paper is organized as follows. The blind equalization model of MQAM is shown in Section II. In Section III, the signal pre-equalization principle and feasibility analysis are presented. Constellation type identification based on template matching is introduced in Section IV. The WXA algorithm is introduced in Section V. In Section VI, extensive simulations are given to evaluate the bind equalization performance. Finally, Section VI shows the main research findings of this paper.

II. System Model

After the signal is modulated and the transmitted over a frequency-selective fading channel [20]-[21]. The received baseband signal for blind equalization can be expressed as

$$y(t) = r(t) + n(t) = \sum_{i=0}^{L-1} h_i \times x(t - \tau_i) + n(t), \quad 0 \le t \le NT_s, \tag{1}$$

where L represents the number of multipath components, h_i and τ_i are the attenuation coefficient and relative delay of the i-th path of the multipath channel, respectively, h_i follows a Rayleigh distribution, $n(t)$ stands for the additive white Gaussian noise with zero mean and a variance of σ^2, $x(t)$ denotes MQAM signal sent by the transmitter, which is expressed as

$$x(t) = P \sum_{k} c_k g(t - kT_s), \tag{2}$$

where P denotes the power normalization factor, M represents the modulation order of the MQAM signal, T represents the constellation shape of the MQAM signal (including square/cross, 110C circular and QCI circular), c_k is the equivalent baseband sequence, T_s is the symbol period, and $g(t)$ stands for the shaping pulse function. The baseband signals referred to herein are normalized to have a unit power. The constellation diagram represents the distribution of the end points of the signal vector, which can be used to visually represent the multi-ary digital modulation signals.

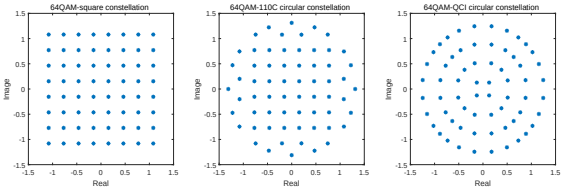

Fig. 1. 64QAM constellation diagrams with different shapes

The MQAM-110C modulation uses a circular constellation mapping to achieve a better peak-to-average ratio without sacrificing the square constellation's pseudo-Gray code characteristics. At the same time, the number of modulus values of the constellation corresponding to MQAM-QCI modulation is relatively small, which can better resist nonlinear distortion in communications. Taking 64QAM as an example, the constellation diagrams with different shapes are shown in Fig. 1.

III. Pre-equalization

A. Constant Modulus Algorithm

The CMA blind equalization algorithm falls into the Bussgang category. This algorithm uses the steepest gradient descent method. The equalizer's tap coefficients are continuously adjusted during each iteration until it converges to minimize the cost function value. In the construction of the cost function, high-order statistics of the received signal are utilized, and the CMA is applied to the signal with a constant envelope, i.e., the normal mode signal.

In the CMA algorithm, $x(n)$ denotes the signal transmitted by the transmitter, $h(n)$ is the impulse of the channel and its length is m. $n(n)$ stands for the zero-mean additive white Gaussian noise with power σ^2, and $y(n)$ is the input signal of the equalizer, $w(n)$ represents the tap coefficient of the blind equalization system, $\tilde{x}(n)$ is the output of the blind equalization system, and $\hat{x}(n)$ is the output of the decoder. The weighting vector of the equalizer is $w(n)$ of length $2L+1$ and its vector form is written as

$$W(n) = [w_{-L}(n), ..., w_0(n), ..., w_L(n)]^T. \tag{3}$$

Let $X(n) = [x(n), ..., x(n-m+1)]^T$, $Y(n) = [y(n+L), ..., y(n) ..., y(n-L)]^T$, then

$$y(n) = \sum_{i=1}^{M-1} c_i x(n-i) + n(n) = C^T X(n) + n(n), \tag{4}$$

and

$$\tilde{x}(n) = \sum_{i=1}^{M-1} w_i y(n-i) = W^T Y(n) = Y^T(n) W(n). \tag{5}$$

In the CMA, the error function can be expressed as

$$e(n) = |\tilde{x}(n)|^2 - R^2, \tag{6}$$

where

$$R^2 = \frac{\mathrm{E}\left\{|x(n)|^4\right\}}{\mathrm{E}\left\{|x(n)|^2\right\}}. \tag{7}$$

The cost function of CMA is expressed as

$$J_{CMA} = \mathrm{E}\left[e^2(n)\right]. \tag{8}$$

The stochastic gradient adaptive algorithm is used to adjust the equalizer's tap coefficients to minimize the cost function. The iteration of equalizer tap coefficient is

$$w_{k+1}(n) = w_k(n) - \mu \hat{\nabla} J_{CMA}(n), \tag{9}$$

where μ represents the iteration depth, and $\hat{\nabla} J_{CMA}(n)$ is the instantaneous value after the derivation, and we have

$$\begin{aligned}
\nabla J_{CMA} &= \frac{\partial J_{CMA}}{\partial w_k(n)} \\
&= \mathrm{E}\left[2\left(|\tilde{x}(n)|^2 - R^2\right)\frac{\partial\left[\tilde{x}(n)\tilde{x}^*(n)\right]}{\partial W(n)}\right] \\
&= \mathrm{E}\left[2\left(|\tilde{x}(n)|^2 - R^2\right)\frac{\partial\left[W^T Y(n)\left(W^T Y(n)\right)^*\right]}{\partial W(n)}\right] \\
&= \mathrm{E}\left[4\left(|\tilde{x}(n)|^2 - R^2\right)Y^*(n)Y^T(n)W(n)\right] \\
&= \mathrm{E}\left[4\left(|\tilde{x}(n)|^2 - R^2\right)Y^*(n)\tilde{x}(n)\right].
\end{aligned} \tag{10}$$

Therefore, the instantaneous value after derivation is

$$\hat{\nabla} J_{CMA} = 4\left(|\tilde{x}(n)|^2 - R^2\right)Y^*(n)\tilde{x}(n), \tag{11}$$

and the tap coefficient iteration is given by

$$\begin{aligned}
w_{k+1}(n) &= w_k(n) - 4\mu\left(|\tilde{x}(n)|^2 - R^2\right)Y^*(n)\tilde{x}(n) \\
&= w_k(n) - 4\mu e(n) Y^*(n)\tilde{x}(n).
\end{aligned} \tag{12}$$

The convergence performance of the equalizer can be measured by the mean squared error (MSE), which reflects the reliability of the output signal of the equalizer. The iterative process is expressed as

$$MSE(n+1) = \eta MSE(n) + (1-\eta)|y(n) - \hat{y}(n)|^2, \tag{13}$$

where η is a forgetting factor, which is greater than 0 and less than 1, generally taking $\eta = 0.99$.

B. Pre-equalization Scheme

The CMA algorithm's universality is powerful, but due to its simplicity, the residual mean square error after convergence is large. In the CMA, a priori information of the transmitted data $x(n)$ is used. The error function is set to

$$e(n) = |\tilde{x}(n)|^2 - R^2, \tag{14}$$

where $R^2 = \mathrm{E}\left\{|x(n)|^4\right\} \Big/ \mathrm{E}\left\{|x(n)|^2\right\}$. Signal set of this paper is Φ={16QAM-square, 16QAM-110C circular, 16QAM-QCI circular, 32QAM-cross, 32QAM-110C circular, 64QAM-square, 64QAM-110C circular, 64QAM-QCI circular}. For these signals, the normalized R^2 of the respective constellations are shown in Table I.

TABLE I
NORMALIZED R^2 OF THE DIFFERENT TYPE CONSTELLATIONS

Constellation type	R^2	$\left\|R^2 - {R_{pre}}^2\right\|$
16QAM-square	0.7333	0.089
16QAM-110C circular	0.9630	0.140
16QAM-QCI circular*	0.9683	0.145
32QAM-cross	0.7706	0.052
32QAM-110C circular	0.8608	0.037
64QAM-square*	0.5918	0.231
64QAM-110C circular	0.7800	0.042
64QAM-QCI circular	0.8302	0.007

From Tab. I, it can be seen that, although the R^2 of MQAM signals of different constellation types are different, they are

roughly distributed in a specific interval. The purpose of pre-equalization is to minimize the multipath interference and recover the shape of the constellation diagram to a large extent without recovering the low residual mean square error. Before the pre-equalization, the receiver has no a priori information, such as the signal's type and statistical characteristics. Therefore, in the parameter setting of the pre-equalizer, we use the "gymnastic scoring method" to remove a maximum value and a minimum value and then take the average value, which gives

$$R_{pre}^2 = 0.823. \tag{15}$$

The pre-equalization idea is to take advantage of the similar statistical characteristics of the QAM. In the parameter setting, the QAM constellation of different shapes can be matched with fixed parameters to counteract the most significant multipath in the recevied signal. Although the parameter mismatch leads to slow convergence and large residual mean square error, the purpose of pre-equalization is to restore the shape of the constellation for subsequent constellation type identification.

IV. Constellation Identification based on Template Matching

A. Template-based Image Matching

Template-based image matching is often referred to as template matching. This matching maps the template onto the reference image, then compares the two images and selects a match based on the dissimilarity or similarity. If the template image set is $A = \{a_1, a_2, ..., a_u\}$ and the reference image set is $B = \{b_1, b_2, ..., b_v\}$. The template matching uses the similarity measurement criterion defined as

$$a_0 = \arg\max_{T \in U_T} S\left(A, T\left(b_i\right)\right), a_o \in A, b_i \in B, \tag{16}$$

and also uses the dissimilarity measurement criterion defined as

$$a_0 = \arg\min_{T \in U_T} D\left(A, T\left(b_j\right)\right), a_o \in A, b_j \in B, \tag{17}$$

where S represents a similarity measure function between the calculation template A and the reference map B, D denotes a difference measure function between the calculation template A and the reference map B, T is a geometric transformation of the image, and U is a transformation space. Therefore, template-based image matching can be described as finding the optimal template to maximize the similarity between the template and the reference image and minimize the difference.

B. Constellation Recognizer Design

The block diagram of the constellation recognizer design based on the similarity criterion and the difference criterion is shown in Fig. 2. The difference or similarity measures refer to the difference or similarity respectively between the calculated template and the reference image in template-based image matching. In this paper, the template image is a standard constellation of 16/32/64QAM, and the reference image is the pre-equalized constellation. Set the template image (standard constellation) a_u to point set $\{p_{u1}, p_{u2}, ..., p_{uM}\}$, where p_{ui} represents the i-th constellation point in the u-th template image, and M is the modulation order of the u-th template image (the number of constellation points), $u = 1, 2, ..., 8$. Let the reference image (pre-equalized constellation) b be the point set $\{q_1, q_2, ..., q_N\}$, where q_j represents the j-th constellation point in the reference image to be classified and N is the number of constellation points sent to the constellation classifier, $j = 1, 2, ..., N$.

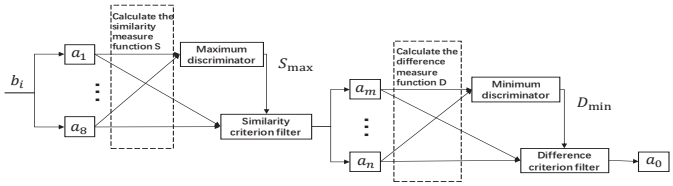

Fig. 2. Constellation recognizer based on similarity criterion and difference criterion

1) Similarity Measure Function Setting: We introduce the specific steps of the similarity measure function S setting as follows:

- Divide the constellation points into M categories according to the minimum distance criterion by

$$p_{uo} = \arg\min \left|p_{uj} - q_i\right|, \tag{18}$$

where p_{uo} denotes the class to which constellation point q_i belongs in the standard constellation.

- Calculate S_i of each point q_i by

$$S_i = \frac{\min\{d\left(k', i\right)\} - r\left(i\right)}{\max\{r\left(k\right), \min\{d\left(k', i\right)\}\}}. \tag{19}$$

Let q_i be divided into the k-th class, which indicates that the corresponding class is p_{uk}. $d\left(k', i\right)$ is the average distance of the i-th point q_i and all signal points divided into the k'-th class, k' is the variable and $k' \neq k$, $r\left(i\right)$ stands for the average distance between the i-th constellation point q_i and other constellation points under the same class.

- Calculate the average of all points S_i in the p_{uk} class S_k by

$$S_k = \frac{\sum\limits_{q_i \in p_{uk}} S_i}{N_k}, \tag{20}$$

where N_k represents the number of sample points in class p_{uk}.

- Calculate the mean of all S_k by

$$S = \frac{1}{M} \sum_{k=1}^{M} S_k. \tag{21}$$

2) Dissimilarity Measure Function Setting: We introduce the specific steps of the dissimilarity measure function D setting as follows:

- Divide the constellation points into M categories according to the minimum distance criterion, which is expressed as

$$p_{uo} = \arg\min \left|p_{uj} - q_i\right|, \tag{22}$$

where p_{uo} is the class to which the constellation point q_i belongs in the standard constellation.

- Calculate D_k of each p_{uk} class by

$$D_k = \frac{\underset{q_i \in p_{uk}}{d}(q_i, p_{uk})}{cul_k}, \tag{23}$$

where $\underset{q_i \in p_{uk}}{d}(q_i, p_{uk})$ is the distance between all points in class p_{uk} and p_{uk} itself, and cul_k represents the number of constellation points contained in class p_{uk}.

- Calculate the sum of all D_k classes D by

$$D = \frac{1}{M}\sum_{k=1}^{M} D_k. \tag{24}$$

3) Decision Criteria Setting: We introduce the specific steps of the judgment criteria setting as follows:

- According to the similarity measure, which is expressed as

$$\{A'\} = \underset{T \in U_T}{\arg} \left(\left|S\left(A', T\left(b_i\right)\right) - \max\left(S\left(A, T\left(b_i\right)\right)\right)\right| < \varepsilon\right) \quad A' \subset A, b_i \in B, \tag{25}$$

where $T\left(b_i\right)$ is power normalization, ε denotes the decision threshold and A' stands for the standard constellation atlas.

- According to the difference measure, which is expressed as

$$\{a_0\} = \underset{T \in U_T}{\arg\min} D\left(A', T\left(b_i\right)\right), \mathrm{a}_0 \in A', b_i \in B, \tag{26}$$

where a_0 is the final decision.

V. Blind Equalization Algorithm and Its Parameter Selection

This section describes the proposed WXA with better performance but higer sensitivity to parameters. Different parameters are selected for different normalized standard constellations so that the residual MSE can converge to a smaller value.

A. Weighted Cross Algorithm

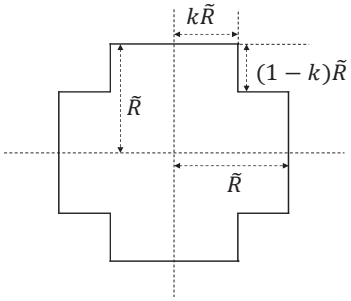

Fig. 3. Cross-shaped modulus curve of CXA

The WXA is based on the CXA [18] and the corresponding modulus curve is shown in Fig. 3. The cross mode is expressed as

$$\frac{1}{2}\left(|kX+Y| + |kX-Y| + |X+kY| + |X-kY| - |X+Y| - |X-Y|\right) = k\tilde{R}, \tag{27}$$

where $\tilde{R} > 0, 0 < k < 1$. According to the cross-shaped modulus curve, the cost function of CXA is

$$J_{CXA} = \frac{1}{4}\mathrm{E}\left[\left(Z_y^2 - 4R^2\right)^2\right], \tag{28}$$

where $R = k\tilde{R}$, Z_y is a function of the equalizer output value $y\left(n\right)$, which is defined as

$$Z_y = |ky_{R,n} + y_{I,n}| + |ky_{R,n} - y_{I,n}| + |y_{R,n} + ky_{I,n}| + |y_{R,n} - ky_{I,n}| - |y_{R,n} + y_{I,n}| - |y_{R,n} - y_{I,n}|, \tag{29}$$

where $y_{R,n}$ and $y_{I,n}$ are the real and imaginary parts of $y\left(n\right)$ respectively.

According to the cross-shaped modulus curve graph and its expression, the CXA has a fixed cross-shaped modulus improved by [18]. The definition of the modulus value incorporates both the constant modulus and the equalizer output value. The decision symbol makes the modulus used by the algorithm better match the cross-shaped constellation. This algorithm is SCXA, whose cost function is written as

$$J_{CXA} = \frac{1}{4}\mathrm{E}\left[\left(Z_y^2 - 2Z_{\hat{y}}R\right)^2\right], \tag{30}$$

where

$$Z_{\hat{y}} = |k\hat{y}_{R,n} + \hat{y}_{I,n}| + |k\hat{y}_{R,n} - \hat{y}_{I,n}| + |\hat{y}_{R,n} + k\hat{y}_{I,n}| + |\hat{y}_{R,n} - k\hat{y}_{I,n}| - |\hat{y}_{R,n} + \hat{y}_{I,n}| - |\hat{y}_{R,n} - \hat{y}_{I,n}|. \tag{31}$$

The k and R values in the above two blind equalization algorithms for the cross-type constellation are constant. Compared to the CXA, the SCXA considers the received signal's instantaneous information to achieve a lower residual MSE. However, the cross-shaped modulus values used by the SCXA remain unchanged during the convergence process, which limits the performance of the algorithm. The cost function of the blind equalizer is expressed as

$$J_{WXA} = \frac{1}{4}\mathrm{E}\left[\left(Z_y^2 - 2^{2-\lambda}Z_{\hat{y}}^{\lambda}R\right)^2\right], \tag{32}$$

where λ is the index weight and $0 < \lambda < 2$. The cost function is based on the following modulus values

$$\frac{1}{2}Z_y = \sqrt{2^{-\lambda}Z_{\hat{y}}^{\lambda}R}, \tag{33}$$

where R denotes the statistical information of the constellation diagram, $Z_{\hat{y}}$ is the contribution of the decision symbol to the modulus value. At different stages of the iteration, the values of λ differ so that the decision symbols contribute differently to the modulus values. At the initial iteration, the equalizer output symbol reliability is low, the contribution to the modulus value should be appropriately reduced, the mean square error is continuously reduced, the output symbol

reliability is increased, and the contribution to the modulus value is increased. The cost function is WXA, which uses both the statistical information of the constellation points and the output of the equalizer. For deriving the WXA equalizer tap iteration formula, this paper derives the partial derivative of the cost function according to the steepest gradient descent method and obtains the iterative formula as follows

$$w_{k+1}(n) = w_k(n) - \mu\left(Z_y^2 - 2^{2-\lambda} Z_{\hat{y}}^{\lambda} R\right) Z_y (X + jY)\, x(n)^*, \tag{34}$$

where μ represents the iteration step size.

$$\begin{aligned} X =& k\mathrm{sgn}\left|ky_{R,n} + y_{I,n}\right| + k\mathrm{sgn}\left|ky_{R,n} - y_{I,n}\right| \\ &+ \mathrm{sgn}\left|y_{R,n} + ky_{I,n}\right| + \mathrm{sgn}\left|y_{R,n} - ky_{I,n}\right| \\ &- \mathrm{sgn}\left|y_{R,n} + y_{I,n}\right| - \mathrm{sgn}\left|y_{R,n} - y_{I,n}\right|, \end{aligned} \tag{35}$$

and

$$\begin{aligned} Y =& \mathrm{sgn}\left|ky_{R,n} + y_{I,n}\right| + \mathrm{sgn}\left|ky_{R,n} - y_{I,n}\right| \\ &+ k\mathrm{sgn}\left|y_{R,n} + ky_{I,n}\right| + k\mathrm{sgn}\left|y_{R,n} - ky_{I,n}\right| \\ &- \mathrm{sgn}\left|y_{R,n} + y_{I,n}\right| - \mathrm{sgn}\left|y_{R,n} - y_{I,n}\right|. \end{aligned} \tag{36}$$

To solve the parameters in the WXA, we assume that the noise is zero, the one-tap equalizer. Let $\frac{\partial J_{WXA}}{\partial d}\big|_{d=1}$ be 0, one has

$$R = \frac{k^5 - k + 1}{k^{3+\lambda} - k + 1} \frac{\mathrm{E}\left[s_R^4\right]}{\mathrm{E}\left[\left|s_R\right|^{2+\lambda}\right]}, \tag{37}$$

The optimal k minimizes the MSE, and the MSE of the algorithm with the cost function is expressed as

$$\varepsilon = \mu P_x \left.\frac{\mathrm{E}\left[\left|\phi(y)\right|^2\right]}{\mathrm{E}\left[\nabla_{y*y} g(y)\right]}\right|_{y=s}, \tag{38}$$

where

$$P_x = \mathrm{E}\left[\|s\|_2^2\right], \tag{39}$$

$$\phi(y) = \nabla_{y^*} J = \left(\frac{\partial}{\partial y_R} + j\frac{\partial}{\partial y_I}\right) J, \tag{40}$$

and

$$g(y) = 2\,\mathrm{Re}\left[\phi(y)(y-s)^*\right]. \tag{41}$$

Substituting the cost function J_{WXA}, we obtain

$$\begin{aligned} \varepsilon_{WXA} = 4\mu P_x \big(& G_1 \mathrm{E}\left[s_R^6\right] - 2G_2 R \mathrm{E}\left[\left|s_R\right|^{4+\lambda}\right] \\ &+ G_3 R^2 \mathrm{E}\left[\left|s_R\right|^{2+2\lambda}\right]\Big) \Big/ 3G_4 \mathrm{E}\left[s_R^2\right] - G_5 R \mathrm{E}\left[\left|s_R\right|^{\lambda}\right], \end{aligned} \tag{42}$$

where $G_1 = k^9 - k + 1$, $G_2 = k^{7+\lambda} - k + 1$, $G_3 = k^{5+2\lambda} - k + 1$, $G_4 = k^5 - k + 1$, $G_5 = k^{3+\lambda} - k + 1$. The optimal k value is expressed as

$$k_{opt} = \arg\min_k \left\{\varepsilon_{WXA}\right\}. \tag{43}$$

From the above analysis, it can be seen that the adaptive adjustment of the parameters at different stages of the equalization determines the performance of the algorithm to a certain extent. The residual MSE reflects the credibility of the equalizer output signal. Therefore, this paper uses MSE adaptive control. The iterative formula for MSE is

$$MSE(n+1) = \eta MSE(n) + (1-\eta)\left|y(n) - \hat{y}(n)\right|^2, \tag{44}$$

where $0 < \eta < 1$, generally take $\eta = 0.99$. The relationship between MSE and λ is difficult to derive. In general, a larger MSE indicates that the equalizer's output is less reliable, and the λ value at this time should be relatively small. This paper assumes a simple linear function to represent the inverse relationship with MSE and λ, which can be expressed as

$$\lambda(n) = -a\left(MSE(n) + b\right), \tag{45}$$

where a is a positive number, and the value of λ should be strictly limited between 0 and 2. In addition, when $k = 1$, the cross-shaped modulus curve evolves into a square. We consider the square as a particular case of the cross star. The WXA can be applied to the cross-shaped QAM constellation and the square QAM constellation.

B. Parameter Selection of the Equalization Algorithm

Although the WXA has universality, it is sensitive to parameters, and different constellations need to converge to different modulus values to obtain a small residual MSE. In this paper, the parameters are solved for constellation diagrams of different shapes, and the corresponding parameters are selected.

1) Parameters k and R Selection: Calculate the optimal k value according to (37), (42), and (43), and then substitute (37) to find the corresponding R value. The k of the square constellation is always 1, and the optimal values of k and R for constellations of different shapes are shown in Table II, Table III, and Table IV.

TABLE II
THE OPTIMAL VALUES OF k AND R FOR 16QAM CONSTELLATION

16 S	λ	0	0.1	0.2	0.3	0.4	0.5	0.6	0.7	0.8	0.9	
	k	1	1	1	1	1	1	1	1	1	1	
	R	0.73	0.74	0.76	0.77	0.79	0.80	0.81	0.83	0.84	0.86	
	λ	1	1.1	1.2	1.3	1.4	1.5	1.6	1.7	1.8	1.9	1.99
	k	1	1	1	1	1	1	1	1	1	1	1
	R	0.87	0.88	0.9	0.91	0.92	0.93	0.95	0.96	0.97	0.98	0.99
16 C	λ	0	0.1	0.2	0.3	0.4	0.5	0.6	0.7	0.8	0.9	
	k	0.99	0.99	0.99	0.99	0.99	0.99	0.99	0.99	0.99	0.99	
	R	0.94	0.95	0.95	0.95	0.96	0.96	0.97	0.97	0.97	0.98	
	λ	1	1.1	1.2	1.3	1.4	1.5	1.6	1.7	1.8	1.9	1.99
	k	0.99	0.99	0.99	0.99	0.99	0.99	0.99	0.99	0.99	0.99	0.99
	R	0.98	0.98	0.99	0.99	0.99	0.99	0.99	1.00	1.00	1.00	1.00
16 Q	λ	0	0.1	0.2	0.3	0.4	0.5	0.6	0.7	0.8	0.9	
	k	0.99	0.99	0.99	0.99	0.99	0.99	0.99	0.99	0.99	0.99	
	R	0.95	0.95	0.96	0.96	0.96	0.97	0.97	0.97	0.98	0.98	
	λ	1	1.1	1.2	1.3	1.4	1.5	1.6	1.7	1.8	1.9	1.99
	k	0.99	0.99	0.99	0.99	0.99	0.99	0.99	0.99	0.99	0.99	0.99
	R	0.98	0.99	0.99	0.99	0.99	0.99	1.00	1.00	1.00	1.00	1.00

2) Parameters a and b setting: According to (45), since $\lambda(n) = -a\left(MSE(n) + b\right)$ and $\lambda(0) \geq 0, a > 0$, one has $MSE(0) + b \leq 0$, or

$$b \leq -MSE(0). \tag{46}$$

TABLE III
THE OPTIMAL VALUES OF k AND R FOR 32QAM CONSTELLATION

32 S	λ	0	0.1	0.2	0.3	0.4	0.5	0.6	0.7	0.8	0.9	
	k	0.97	0.97	0.97	0.96	0.96	0.96	0.96	0.95	0.95	0.95	
	R	0.73	0.74	0.75	0.76	0.77	0.79	0.80	0.81	0.82	0.84	
	λ	1	1.1	1.2	1.3	1.4	1.5	1.6	1.7	1.8	1.9	1.99
	k	0.95	0.95	0.95	0.95	0.95	0.95	0.95	0.95	0.95	0.95	0.95
	R	0.85	0.87	0.88	0.90	0.91	0.93	0.94	0.95	0.97	0.98	1.00
32 C	λ	0	0.1	0.2	0.3	0.4	0.5	0.6	0.7	0.8	0.9	
	k	0.98	0.97	0.97	0.97	0.97	0.96	0.96	0.96	0.96	0.96	
	R	0.82	0.83	0.83	0.84	0.85	0.86	0.87	0.88	0.89	0.90	
	λ	1	1.1	1.2	1.3	1.4	1.5	1.6	1.7	1.8	1.9	1.99
	k	0.96	0.96	0.96	0.96	0.96	0.96	0.96	0.96	0.96	0.96	0.96
	R	0.91	0.92	0.93	0.94	0.95	0.96	0.96	0.97	0.98	0.99	1.00

TABLE IV
THE OPTIMAL VALUES OF k AND R FOR 64QAM CONSTELLATION

64 S	λ	0	0.1	0.2	0.3	0.4	0.5	0.6	0.7	0.8	0.9	
	k	1	1	1	1	1	1	1	1	1	1	
	R	0.59	0.61	0.63	0.65	0.67	0.69	0.71	0.73	0.75	0.77	
	λ	1	1.1	1.2	1.3	1.4	1.5	1.6	1.7	1.8	1.9	1.99
	k	1	1	1	1	1	1	1	1	1	1	1
	R	0.79	0.81	0.83	0.85	0.87	0.89	0.91	0.94	0.96	0.98	1.00
64 C	λ	0	0.1	0.2	0.3	0.4	0.5	0.6	0.7	0.8	0.9	
	k	0.97	0.97	0.96	0.96	0.96	0.95	0.95	0.95	0.95	0.95	
	R	0.74	0.75	0.76	0.77	0.78	0.79	0.80	0.82	0.83	0.84	
	λ	1	1.1	1.2	1.3	1.4	1.5	1.6	1.7	1.8	1.9	1.99
	k	0.95	0.95	0.94	0.94	0.94	0.94	0.94	0.94	0.94	0.94	0.94
	R	0.86	0.87	0.88	0.90	0.91	0.93	0.94	0.96	0.97	0.99	1.00
64 Q	λ	0	0.1	0.2	0.3	0.4	0.5	0.6	0.7	0.8	0.9	
	k	0.97	0.97	0.97	0.96	0.96	0.96	0.96	0.96	0.96	0.95	
	R	0.79	0.80	0.80	0.81	0.82	0.83	0.84	0.85	0.86	0.88	
	λ	1	1.1	1.2	1.3	1.4	1.5	1.6	1.7	1.8	1.9	1.99
	k	0.95	0.95	0.95	0.95	0.95	0.95	0.95	0.95	0.95	0.95	0.95
	R	0.89	0.90	0.91	0.92	0.93	0.94	0.96	0.97	0.98	0.99	1.00

Set the convergence MSE of the CMA to the expected MSE of the algorithm, denoted as $MSE\,(\text{end})$, then one has

$$a \leq \frac{-\lambda\,(\text{end})}{MSE\,(\text{end}) + b}, \tag{47}$$

where $\lambda\,(\text{end}) = 2$.

In this paper, the parameter values are determined according to different modulation orders, as shown in Table V.

TABLE V
THE VALUES OF a AND b OF DIFFERENT SHAPE CONSTELLATIONS OF DIFFERENT MODULATION ORDERS

parameter	16QAM			32QAM		64QAM		
	square	110C	QCI	cross	110C	square	110C	QCI
MSE(0)	0.05	0.05	0.05	0.025	0.025	0.015	0.015	0.015
MSE(end)	0.01	0.01	0.01	0.01	0.01	0.003	0.003	0.003
b	-0.06	-0.06	-0.06	-0.04	-0.04	-0.02	-0.02	-0.02
a	40	40	40	66.67	66.67	117.64	117.64	117.64

C. MQAM Blind Equalization Steps with Unknown Constellation

This section introduces WXA that improves the CXA and SCXA by matching different constellation shape parameters so that the residual MSE can converge to a smaller value. In summary, the steps of the MQAM blind equalization algorithm for the unknown constellation type proposed in this paper are given in Algorithm 1.

Algorithm 1 The steps of blind equalization with unknown constellation for MQAM.

1: Setting parameters and use the CMA algorithm to pre-equalize the MQAM with the unknown constellation type;
2: Solve the parameters of the converged constellation points according to (25) and (26), and use Fig. 4 to identify different types of 16/32/64QAM constellation;
3: According to the recognition results, different parameters are matched and the constellations are equalized by the WXA algorithm.

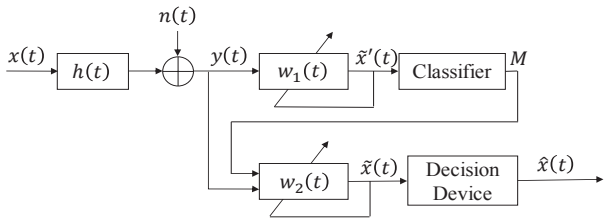

Fig. 4. MQAM constellation identification and blind equalization parameter selection process

VI. SIMULATION RESULTS AND DISCUSSION

To demonstrate our proposed method's effectiveness and superiority, we conduct simulations and present the results in this section. Different constellation types of MQAM are considered, including square 16QAM, 110C circular 16QAM, QCI circular 16QAM, cross 32QAM, 110C circular 32QAM, square 64QAM, 110C circular 64QAM, and QCI circular 64QAM. The simulation parameters used are: the symbol rate of the signal is 1M Baud/s, the over-sampled multiple is 8, and the raised cosine roll-off filter with the roll-off factor of 0.35 [22]. The number of transmitted symbols is 160000, the number of Monte Carlos is 3000, the frequency selective fading channels are ITU_I_A in Rec. ITU-R M. 225 and ITU_I_B in Rec. ITU-R M. 225 and the channel parameters are shown in VI and VII [23].

TABLE VI
CHANNEL PARAMETER OF ITU_I_A

Path Index	Delay (ns)	Power gain (dB)
1	0	0
2	50	-3
3	110	-10
4	170	-18
5	290	-26
6	310	-32

A. Pre-equalization

TABLE VII
CHANNEL PARAMETER OF ITU_I_B

Path Index	Delay (ns)	Power gain (dB)
1	0	0
2	100	-3.6
3	200	-7.2
4	300	-10.8
5	500	-18
6	700	-25.2

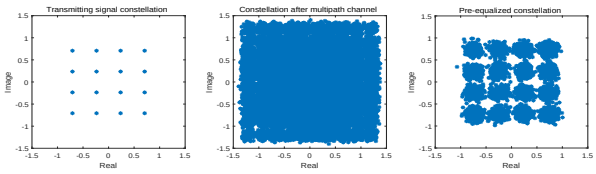

Fig. 5. 16QAM-square constellation pre-equalization over ITU_I_A channel

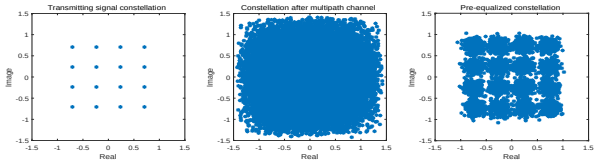

Fig. 6. 16QAM-square constellation pre-equalization over ITU_I_B channel

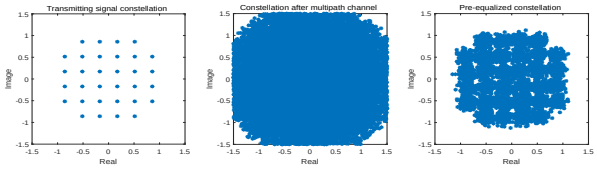

Fig. 7. 32QAM-cross constellation pre-equalization over ITU_I_A channel

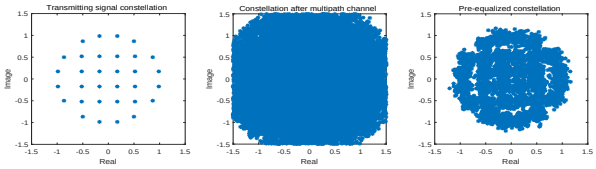

Fig. 8. 32QAM-110C circular constellation pre-equalization over ITU_I_A channel

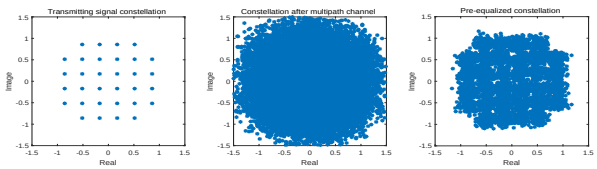

Fig. 9. 32QAM-cross constellation pre-equalization over ITU_I_B channel

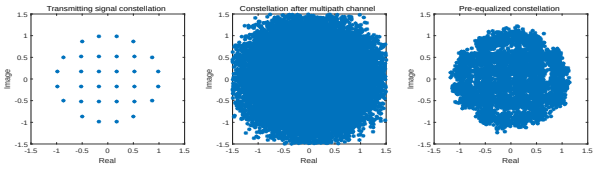

Fig. 10. 32QAM-110C circular constellation pre-equalization over ITU_I_B channel

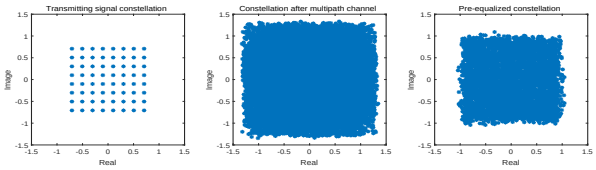

Fig. 11. 64QAM-square constellation pre-equalization over ITU_I_A channel

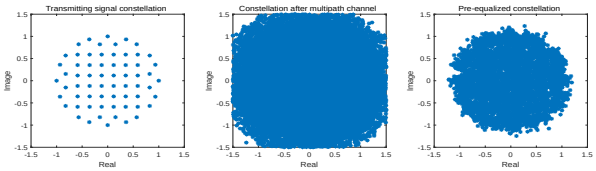

Fig. 12. 64QAM-110C circular constellation pre-equalization over ITU_I_A channel

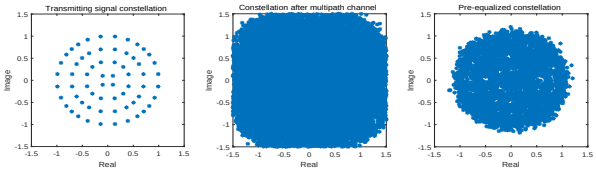

Fig. 13. 64QAM-QCI circular constellation pre-equalization over ITU_I_A channel

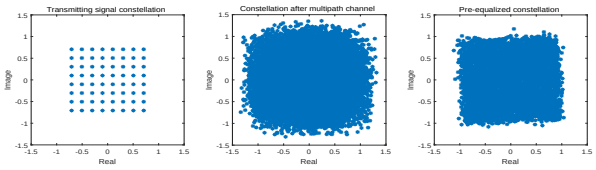

Fig. 14. 64QAM-square constellation pre-equalization over ITU_I_B channel

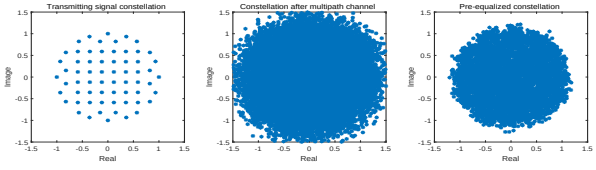

Fig. 15. 64QAM-110C circular constellation pre-equalization over ITU_I_B channel

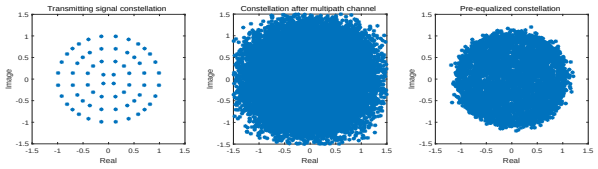

Fig. 16. 64QAM-QCI circular constellation pre-equalization over ITU_I_B channel

Figs. 5-16 show the QAM pre-equalization results with different constellations. The symbol rate of the signal is, the oversampling multiple is 8, and the raised cosine roll-off filter has a roll-off factor of 0.5. The number of transmitted symbols is 160000, and the signal types are square 16QAM, 110C circular 16QAM, QCI circular 16QAM, cross 32QAM, 110C circular 32QAM, square 64QAM, 110C circular 64QAM and QCI circular 64QAM. The channel is the channel ITU_I_A and ITU_I_B in M.225, the SNR is 20dB, and the equalization algorithm uses a fixed-parameter CMA algorithm with a step size of 0.01. These Figs show that the pre-equalization based on the CMA algorithm can roughly restore the constellation's shape for subsequent recognition.

B. MQAM Constellation Identification

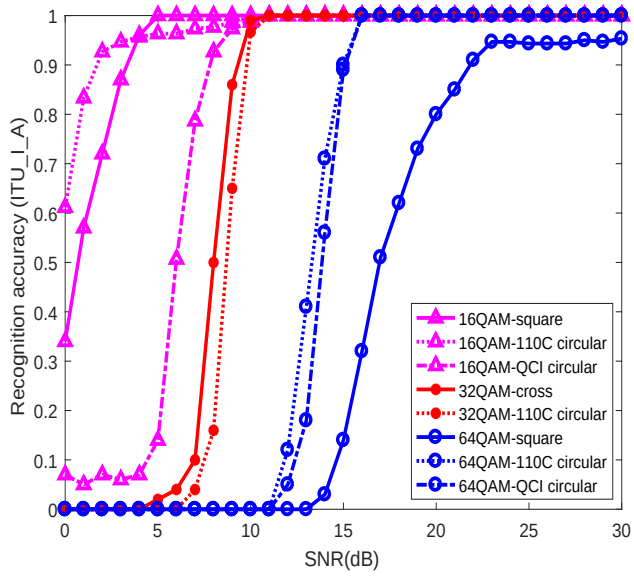

Fig. 17. MQAM constellation identification performance over ITU_I_A channel

The number of transmitted symbols is 160,000. The feature points are extracted from the 5000 samples after the convergence of the residual MSE. The test channel is ITU_I_A in M.225, and the result of the identification of the MQAM constellation identification performance is shown in Fig. 17. The comprehensive similarity measure function and the difference measure function are used to identify eight different QAM constellation identification. From Fig. 17, it can be seen that 16QAM-square and 16QAM-110C circular have a recognition accuracy of more than 90% when the SNR is 4dB, and the recognition accuracy of the 16QAM-QCI circular is more than 90% when the SNR=8dB. 32QAM-Cross, 32QAM-110C circular recognition accuracy rate of more than 90% when the SNR=9dB, 64QAM-110C circular and 64QAM-QCI circular recognition accuracy rates are more than 90% when the SNR is 14dB, the 64QAM-square recognition accuracy rate is over 90% when the SNR is 22dB. The above identification thresholds can satisfy the QAM demodulation threshold proposed in the military standard 110C. Since R^2 of the 16QAM-QCI circular constellation diagram and the 64QAM-square constellation diagram differ significantly from the pre-equalization parameter R^2_{pre}, the remaining inter-symbol interference after pre-equalization is still very large. Compared with other shape constellations under the same modulation order, the recognition accuracy of these two constellations is low, and the experimental results validate the theoretical analysis.

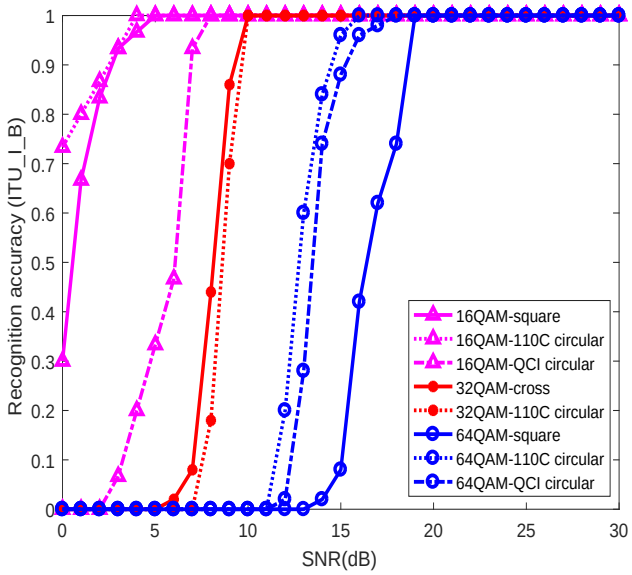

Fig. 18. MQAM constellation identification performance over ITU_I_B channel

Fig. 18 is the constellation identification performance of MQAM over channel ITU_I_B. The number of transmission symbols is 160,000, and the feature quantity is extracted by taking 5000 sampling points after the convergence of the residual MSE, and the channel is the ITU_I_B in Rec. ITU-R M. 225. From Fig. 18, we observe that the recognition accuracy of the 16QAM-square and 16QAM-110C circular are over 90% when SNR=3dB. 16QAM- QCI circular has a recognition accuracy of more than 90% when the SNR is 8dB. 32QAM-cross and 32QAM-110C circular recognition accuracy rate is more than 90% when the SNR is 10dB. 64QAM-110C circular and 64QAM-QCI circular recognition accuracy rate are more than 90% when the SNR is 16dB. 64QAM-square improves the recognition rate to over 90% when SNR=19 dB. The above identification thresholds can satisfy the QAM demodulation threshold proposed in the military standard 110C. R^2 of 16QAM-QCI circular constellation diagram and the 64QAM-square constellation diagram differ

significantly from the pre-equalization parameter R_{pre}^2. After pre-equalization, the remaining inter-symbol interference is still substantial. Compared with other shape constellations under the same modulation order, the recognition accuracy of these two constellations is low, and the experimental results are in line with the theoretical analysis.

C. WXA Parameters Selection and Equalization Results

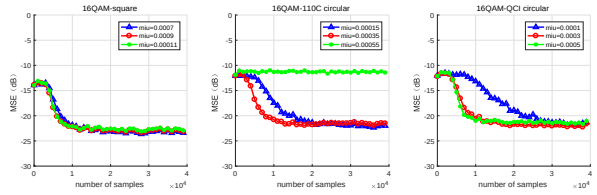

Fig. 19. Different μ selection for 16QAM-square, 110C circular and QCI circular constellation

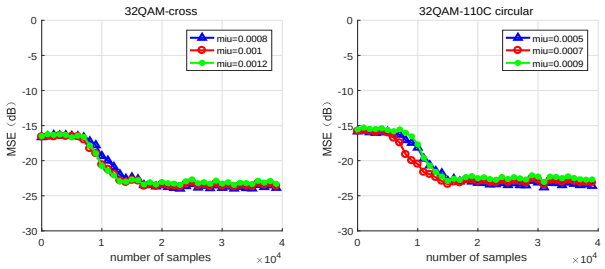

Fig. 20. Different μ selection for 32QAM-cross, 110C circular constellation

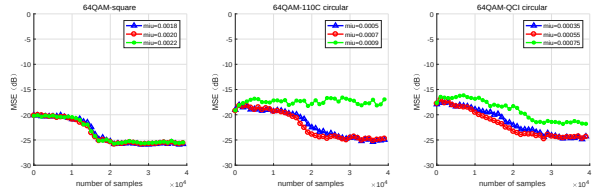

Fig. 21. Different μ selection for 64QAM-square, 110C circular and QCI circular constellation

TABLE VIII
OPTIMAL μ OF DIFFERENT SHAPE CONSTELLATIONS IN WXA

	16QAM			32QAM		64QAM		
Step size	square	110C	QCI	cross	110C	square	110C	QCI
μ	0.0009	0.00035	0.0003	0.001	0.0007	0.002	0.0007	0.00055

Fig. 19-21 are for different the step size of different constellation diagram types. The number of symbols is 40000, and the channel is ITU_I_A in Rec. ITU-R M. 225, the SNR is 20dB. The equalization algorithm is based on the parameter matching WXA algorithm. It sets the non-synchronization length so that the convergence speed is the fastest and the step of the residual MSE is the optimal step size. The 16QAM-square constellation has a convergence speed close to 0.0009, but it converges faster at 0.0009. Therefore, we choose this value as the step size. The 16QAM-110C circular constellation diagram converges at the fastest rate with a step size of 0.00035. The 16QAM-QCI circular constellation diagram converges at the most rapid rate with a step size of 0.003. Thus, these two values are selected as the step size. Similarly, the optimal step size of the WXA algorithm for other modulation orders and constellations are shown in Table VIII.

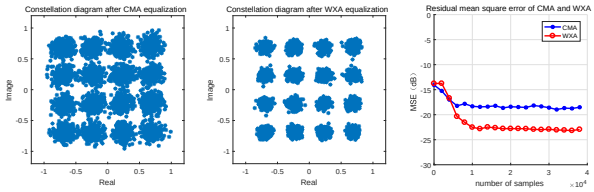

Fig. 22. CMA and WXA comparison of 16QAM-square constellation

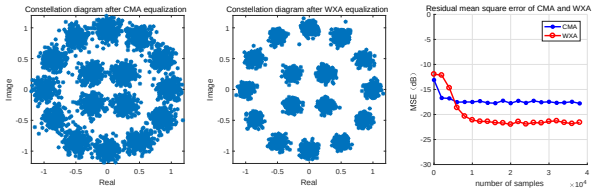

Fig. 23. CMA and WXA comparison of 16QAM-110C circular constellation

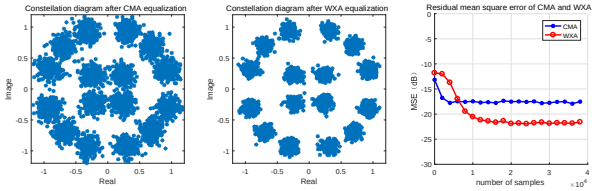

Fig. 24. CMA and WXA comparison of 16QAM-QCI circular constellation

Fig. 22-24 compare the proposed WXA equalization with the CMA for 16QAM. The number of symbols is 80000. The signal types are 16QAM-square, 16QAM-110C, 16QAM-QCI. The channels are ITU_I_A in Rec. ITU-R M. 225 and SNR is 20dB. The equalization algorithm applies the CMA and the parameter matching WXA algorithm, and the step size is the matching step size. From Fig. 22-24, it can be seen that the parameter matching WXA algorithm can well balance the 16QAM with various shape constellation diagrams and achieve convergence at about 2000 points. The residual MSE after stable convergence can reach about -22dB.

The number of symbols is 80000, and the channel is ITU_I_A in Rec. ITU-R M. 225, and SNR is 20 dB. For the 32QAM-cross constellation diagram, the equalization algorithm uses the CMA algorithm, CXA algorithm, SCXA algorithm, and parameter matching WXA algorithm. The step size is matching the step size. The comparison of CMA, CXA, SCXA, and WXA of 32QAM-cross constellation are shown in Fig. 25. It can be observed from Fig. 26 that the convergence speed of the CMA algorithm is the slowest, followed by the CXA algorithm and the SCXA algorithm. The WXA algorithm has the fastest convergence speed, and the residual mean square error of the WXA algorithm is the lowest, which

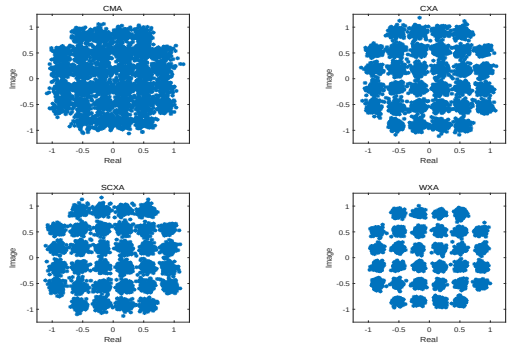

Fig. 25. Equalization performance comparison for CMA, CXA, SCXA and WXA of 32QAM-cross constellation

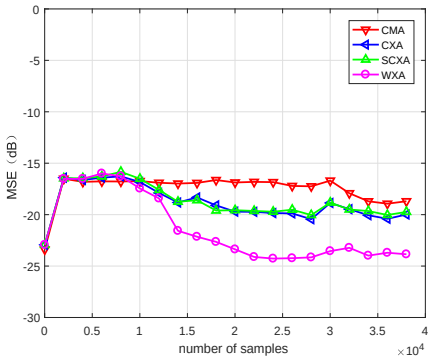

Fig. 26. Convergence speed comparison of CMA, CXA, SCXA and WXA for 32QAM-cross constellation

can reach -26dB. For the 32QAM-110C circular constellation, the equalization algorithm uses the CMA algorithm and the parameter matching WXA algorithm, and the step size is the matching step size. Fig. 27 shows that the CMA algorithm's convergence speed is slow, the convergence speed of the WXA algorithm is fast, and the residual MSE of the WXA algorithm is as low as -26dB. According to the above results, the WXA algorithm with parameter matching can balance the various shape constellations of 32QAM, and the residual MSE after stable convergence can reach -23dB.

Fig. 28-30 show the proposed WXA equalization comparison with the CMA by three constellation results of 64QAM. The number of symbols is 80000. The signal types are 64QAM-square, 64QAM-110C, 64QAM-QCI. The channels are ITU_I_A in Rec. ITU-R M. 225. The SNR is 20dB. The equalization algorithm is based on the CMA algorithm and the parameter matching WXA algorithm. The step size is the matching step size. From Fig. 28-30, it can be observed that the WXA algorithm with parameter matching can well balance the various shape constellations of 64QAM, and the residual MSE after stable convergence can reach -25dB.

The WXA algorithm has the same universality of the constellation of different shapes as the CMA algorithm from the above analysis. However, its equalization effect is better than that of the CMA algorithm. In the case of sacrificing partial convergence speed, a lower residual MSE can be obtained. For the cross-shaped constellation, the convergence speed of the WXA algorithm is almost the same as that of CXA and SCXA, and the WXA algorithm can obtain a smaller residual MSE. Therefore, the proposed WXA algorithm has the constellation shape's universality and can bring a smaller residual MSE.

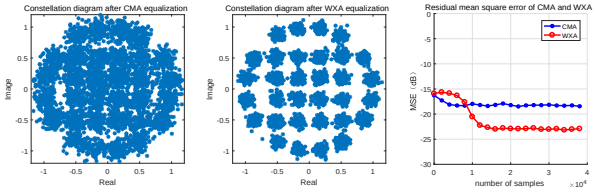

Fig. 27. CMA and WXA comparison of 32QAM-110C circular constellation

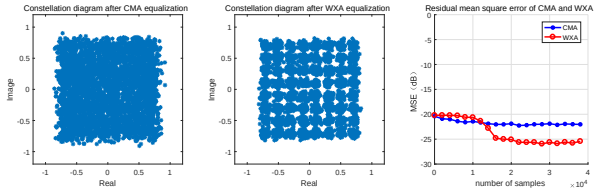

Fig. 28. CMA and WXA comparison of 64QAM-square constellation

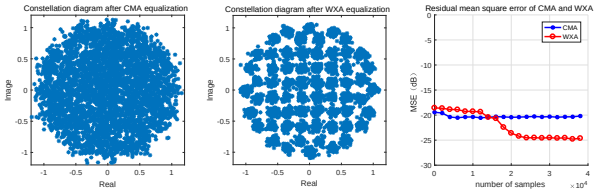

Fig. 29. CMA and WXA comparison of 64QAM-110C circular constellation

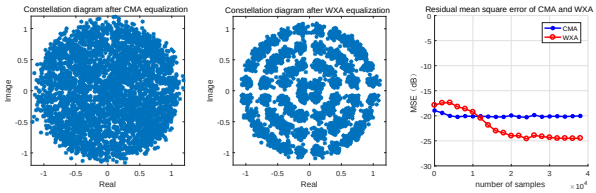

Fig. 30. CMA and WXA comparison of 64QAM-QCI circular constellation

VII. Conclusion

This paper has proposed a novel low-overhead blind equalization method for multiple quadrature amplitude modulation with unknown constellation to combat the frequency-selective fading for air-to-ground multipath UAV communications. The pre-equalization of the constellation was performed firstly, and the contour of the constellation was restored. Secondly, the similarity measurement function and the difference measurement function were established based on the template matching. Thirdly, the constellation diagrams of different shapes of the three modulation orders of 16/32/64QAM were identified. This paper has also introduced a highly universal weighted constant cross algorithm. When constructing the cross-shaped

modulus value, the proposed algorithm utilized the signal constellation points' statistical information and the equalizer output decision symbols' weighting value to achieve a lower residual mean square error. Simulation results show that the signal's correct recognition rate increases with the increase of the signal-to-noise ratio but decreases with the increase of the modulation order. After selecting the corresponding parameters, the proposed weighted constant cross algorithm can reduce the residual mean square error's convergence value to between -22dB and -25dB. As such, the proposed method is beneficial for green air-ground multipath UAV communications.

REFERENCES

[1] W. Wang, J. Tang, N. Zhao, X. Liu, X. Zhang, Y. Chen, Y. Qian, "Joint precoding optimization for secure SWIPT in UAV-Aided NOMA networks," *IEEE Transactions on Communicaitons,* vol. 68, no. 8, pp. 5028-5040, Aug. 2020.

[2] Xi. Pang, J. Tang, N. Zhao, X. Zhang, Y. Qian, "Energy-efficient design for mmWave-enabled NOMA-UAV networks," *Science China-Information Sciences,* 2020, to appear.

[3] M. Liu, K. Yang, N. Zhao, Y. Chen, H. Song, F. Gong, "Intelligent signal classification in industrial distributed wireless sensor networks-based IIoT," *IEEE Transactions on Industrial Informatics,* vol. 17, no. 7, pp. 4946-4956, July 2021.

[4] B. Zheng, L. Deng, M. Sawahashi, N. Kamiya, "High-order circular QAM constellation with high LDPC coding rate for phase noise channels," in *Proc. 20th International Symposium on Wireless Personal Multimedia Communications,* 2017, pp. 196-201.

[5] M. Liu, G. Liao, N. Zhao, H. Song and F. Gong, "Data-driven deep learning for dignal classification in industrial cognitive radio networks," *IEEE Transactions on Industrial Informatics,* vol. 17, no. 5, pp. 3412-3421, May. 2021.

[6] M. Bouchou, H. Wang, M. Lakhdari, "Automatic digital modulation recognition based on stacked sparse autoencoder," in *Proc. 17th International Conference on Communication Technology,* 2017, pp.28-32.

[7] M. Laghate, S. Chaudhari, D. Cabric, "USRP N210 demonstration of wideband sensing and blind hierarchical modulation classification," in *Proc. IEEE International Symposium on Dynamic Spectrum Access Networks,* 2017, pp.1-3.

[8] Y. Zhao, X. Yang, Y. Lin, "A new recognition method for M-QAM signals in software defined radio," in *Proc. IEEE International Conference on Software Quality, Reliability and Security Companion,* 2017, pp.271-275.

[9] H. Ren, J. Yu, Z. Wang, J. Chen, C. Yu, "Modulation format recognition in visible light communications based on higher order statistics," in *Proc. Conference on Lasers and Electro-Optics Pacific Rim,* 2017, pp. 1-2.

[10] L. Wang, Y. Li, "Constellation based signal modulation recognition for MQAM," in *Proc. 9th International Conference on Communication Software and Networks,* 2017, pp. 826-829.

[11] Y. Yadav, G. Jajoo, S. Yadav, "Modulation scheme detection of blind signal using constellation graphical representation," in *Proc. International Conference on Computer, Communications and Electronics,* 2017, pp. 231-235.

[12] P. Priyadarshi, C. Rai, "Blind channel equalization using modified constant modulus algorithm," in *Proc. International Conference on Computing, Communication and Automation,* 2016, pp. 1020-1024.

[13] J. Li, D. Feng, W. Zheng, "An efficient soft decision-directed algorithm for blind equalization of 4-QAM systems," in *Proc. IEEE International Symposium on Circuits and Systems,* 2016, pp. 1726-1729.

[14] J. Li, D. Feng, B. Li, "Space-time blind equalization of dispersive MIMO systems driven by QAM signals," *IEEE Transactions on Vehicular Technology,* vol. 67, no. 5, pp. 4136-4148, May 2018.

[15] Q. Khan, S. Viqar, S. Sheikh, "Two novel blind equalization algorithms for rectangular quadrature amplitude modulation constellations," *IEEE Access,* vol. 4, pp. 9512-9519, Dec. 2016.

[16] R. Yang, L. Yang, J. Zhang, C. Sun, W. Cong, S. Zhu, "Blind equalization of QAM signals via extreme learning machine," in *Proc. 10th International Conference on Advanced Computational Intelligence,* 2018, pp. 34-39.

[17] S. Abrar, "A new cost function for the blind equalization of cross-QAM signals," in *Proc. 17th International Conference on Microelectronics,* 2005, pp. 290-295.

[18] S. Abrar, I. Qureshi, "Blind equalization of cross-QAM signals," *IEEE Signal Processing Letters,*. vol. 13, no. 12, pp.745-748, Dec. 2006.

[19] S. Liu, J. Hu, M. Dai, "Two novel algorithms for blind equalization of cross-QAM signals," in *Proc. International Conference on Communications, Circuits and Systems,* 2008, pp. 905-909.

[20] J. Bae, Y. Kim, N. Hur, H. Kim, "Study on air-to-ground multipath channel and mobility influences in UAV based broadcasting," in *Proc. 2018 International Conference on Information and Communication Technology Convergence,* 2018, pp. 1534-1538.

[21] M. Zaman, S. Mamun, M Gaffar, M. Alam, M. Momtaz, "Modeling VHF air-to-ground multipath propagation channel and analyzing channel characteristics and BER performance," in *Proc. 2010 IEEE Region 8 International Conference on Computational Technologies in Electrical and Electronics Engineering,* 2010, pp. 335-338.

[22] C. Wang, M. Liu, Q. Chen, B. Shang, H. Tang. "Automatic digital modulation recognition in the presence of alpha-stable noise," *Physical Communication,* vol. 43, no. 101221, pp. 1-8, Dec. 2020.

[23] M. Liu, N. Zhao, J. Li and V. Leung, "Spectrum sensing based on maximum generalized correntropy under symmetric alpha stable noise," *IEEE Transactions on Vehicular Technology*, vol. 68, no. 10, pp. 10262-10266, Oct. 2019.